

Quantitative Assessment of Intestinal First-pass Metabolism of Oral Drugs Using Portal-vein Cannulated Rats

Yoshiki Matsuda · Yoshihiro Konno · Takashi Hashimoto · Mika Nagai · Takayuki Taguchi · Masahiro Satsukawa · Shinji Yamashita

Received: 22 April 2014 / Accepted: 15 August 2014 / Published online: 28 August 2014
© Springer Science+Business Media New York 2014

ABSTRACT

Purpose To evaluate the impact of intestinal first-pass metabolism (Fg) by cytochrome P4503A (CYP3A) and uridine 5'-diphosphate-glucuronosyltransferases (UGT) on *in vivo* oral absorption of their substrate drugs.

Methods CYP3A and UGT substrates were orally administered to portal-vein cannulated (PV) rats to evaluate their intestinal availability (Fa·Fg). In the case of CYP3A substrates, vehicle or 1-aminobenzotriazole (ABT), a potent inhibitor of CYP enzymes, was pretreated to assess Fg separately from Fa (Enzyme-inhibition method). On the other hand, since potent inhibitors of UGT have not been identified, Fg of UGT substrate was calculated from total amount of metabolites generated in enterocytes (Metabolite-distribution method).

Results After oral administration of CYP3A substrates in ABT-pretreated rats, the portal and systemic plasma concentrations of the metabolite were nearly the same, indicating almost complete inhibition of intestinal CYP3A-mediated metabolism. Using Enzyme-inhibition method, Fg of midazolam (1 mg/kg) was calculated as 0.71. Additionally, total amount of raloxifene-6-glucuronide generated in enterocytes after oral administration of raloxifene was estimated using Metabolite-distribution method and Fg of raloxifene (0.98 μ mol/kg) was calculated as 0.21.

Conclusions PV rats enabled *in vivo* quantitative assessment of intestinal first-pass metabolism by CYP3A and UGT. This method is useful for clarifying the cause of low bioavailability.

KEY WORDS CYP3A · intestinal metabolism · oral absorption · portal vein-cannulated rats · UGT

ABBREVIATIONS

ABT	1-Aminobenzotriazole
ANT	Antipyrine
BUS	Buspirone
CYP	Cytochrome P450
D-FEL	Dehydrofelodipine
FEX	Fexofenadine
FEL	Felodipine
MDZ	Midazolam
6-OH-BUS	6-Hydroxybuspirone
1-OH-MDZ	1-Hydroxy-midazolam
4-OH-MDZ	4-Hydroxy-midazolam
P-gp	P-glycoprotein
PV rats	Portal vein-cannulated rats
RLX	Raloxifene
R4'G	Raloxifene-4'-glucuronide
R6G	Raloxifene-6-glucuronide
UGT	Uridine 5'-diphosphate –glucuronosyltransferase

INTRODUCTION

Cytochrome P450 3A (CYP3A) subfamily members are involved in approximately 80% of oxidative metabolism and almost 50% of the overall elimination of commonly used drugs [1]. CYP3A is reported to be the most abundant CYP subfamily in the human intestine, where the average content of CYP3A in the enterocyte represents approximately 80% of the total CYP enzyme present [2,3]. After oral administration, many CYP3A substrate drugs, such as midazolam (MDZ), nicardipine and simvastatin, are known to undergo extensive first-pass metabolism in the intestine and show relatively low oral bioavailability in humans [4].

Y. Matsuda (✉) · Y. Konno · T. Hashimoto · M. Nagai · T. Taguchi · M. Satsukawa
Pharmacokinetics and Safety Research Department, Central Research Laboratories, Kaken Pharmaceutical Co., Ltd, 14 Shinomiya Minamigawara-cho, Yamashina-ku, Kyoto 607-8042, Japan
e-mail: matsuda_yoshiki@kaken.co.jp

S. Yamashita
Faculty of Pharmaceutical Sciences, Setsunan University, 45-1 Nagaotobe-cho, Hirakata 573-0101, Osaka, Japan

Uridine 5'-diphosphate (UDP)-glucuronosyltransferases (UGT) are also important drug-metabolizing enzymes in humans, which contribute to the elimination of 10% of the top 200 prescribed drugs [5]. Mizuma *et al.* [6] reported that the extremely low bioavailability of raloxifene (RLX) in humans could be attributed to intestinal first-pass metabolism by UGTs. Therefore, a comprehensive understanding of the contribution of these enzymes to first-pass metabolism in key preclinical animal species would be important for characterizing pharmacokinetics of new chemical entities during the drug discovery and development stage, especially in regard to their oral absorbability.

As awareness of the importance of intestinal first-pass metabolism by CYP3A and UGTs in humans increases, *in vitro* and *in vivo* studies for determining intestinal availability (Fg, fraction not metabolized in the gastrointestinal (GI) tract) are having important roles in the selection of oral drug candidates. Although the use of *in vitro-in vivo* extrapolation to evaluate hepatic metabolism is widely accepted, kinetic models that describe intestinal first-pass metabolism have not been fully validated because the extent of intestinal metabolism is influenced not only by intrinsic metabolic activity but also by physiological complexities that are unique to the GI tract. Ogasawara *et al.* [7] and Nishimuta *et al.* [8] reported an *in vivo* approach to determine the Fg of orally administered drugs based on the inhibitory effect of grapefruit juice or ketoconazole at low dose upon oral exposure. With these approaches, however, if the systemic clearance of the test compound is significantly affected by oral treatment with inhibitors, intravenous studies should be conducted at each inhibitor dose to calculate the exact value for bioavailability.

On the other hand, we have indicated the possibility of using portal-vein cannulated (PV) rats to evaluate oral absorption of drugs independently of variable systemic clearance [9]. With this method, Fa·Fg (Fa, fraction absorbed from the GI tract) of orally administered drugs can be calculated based only on an oral administration study; an intravenous administration study is not required.

As a next step, this study attempted to analyze the individual values of Fa and Fg for CYP3A and UGT substrate drugs. In the case of CYP3A substrate drugs, 1-aminobenzotriazole (ABT), a nonspecific mechanism-based inhibitor of CYP enzymes, was used to assess Fg separately from Fa (Enzyme-inhibition method). Strelevitz *et al.* [10] reported that the pretreatment with ABT at 100 mg/kg significantly decreased systemic clearance of MDZ, CYP3A substrate, in rats as a result of inhibition of CYP-mediated metabolism. ABT has been shown to have no inhibitory effects on phase II drug-metabolizing enzymes such as UGT and sulfotransferase (SULT), although it inhibits N-acetyltransferase (NAT) [11]. Also, ABT showed no

effects on the activity of transporters such as organic anion transporting peptides (OATPs) or P-glycoprotein (P-gp) [10]. In addition, ABT has been demonstrated to be non-toxic in rats even with an acute high dose and multiple dosings [12,13].

On the contrary, since specific and potent inhibitors for UGTs have not been identified, another method for calculating the Fg of UGT substrate drugs was developed in which distribution of metabolites to the intestinal lumen and the mesenteric vein was evaluated with an *in situ* single-pass intestinal perfusion experiment (Metabolite-distribution method). Raloxifene (RLX), a selective estrogen receptor modulator used in the treatment of osteoporosis, has been reported to be converted to raloxifene-6-glucuronide (R6G) by UGT1a in rat hepatic and intestinal microsomes [14]. The R6G generated in enterocytes is transported into both the mesenteric vein and the intestinal lumen by passive and active transport [15,16]. In this study, RLX was used as a UGT substrate model and distribution of R6G was evaluated. In addition, the amount of R6G absorbed from enterocytes after oral administration of RLX was calculated by monitoring the concentration of R6G in portal and systemic plasma and the amount of RLX metabolized in these cells was estimated.

This study is expected to provide a new method using PV rats to evaluate Fa and Fg for several types of drugs and to identify factors which limit oral bioavailability in the drug discovery stage.

MATERIALS AND METHODS

Materials

Fexofenadine (FEX), felodipine (FEL), buspirone (BUS), raloxifene (RLX) and ketoconazole were purchased from Sigma-Aldrich (St. Louis, MO, USA). Midazolam (MDZ) and antipyrine (ANT) were purchased from Wako Pure Chemicals (Osaka, Japan), and 1-aminobenzotriazole (ABT) was purchased from Tokyo Chemical Industry (Tokyo, Japan). 1-OH-midazolam (1-OH-MDZ), 4-OH-midazolam (4-OH-MDZ), dehydrofelodipine (D-FEL), 6-OH-buspirone (6-OH-BUS), raloxifene-4'-glucuronide (R4'G) and raloxifene-6-glucuronide (R6G) were purchased from Toronto Research Chemicals (North York, Canada). All other chemicals used were reagent grade or better.

Animals

All animal procedures were conducted under protocols approved by the Kaken Institutional Animal Care and Use Committee and were performed in accordance with the

Principles of Laboratory Animal Care (NIH publication No. 85–23, revised 1985). Cannulated male Sprague–Dawley rats (8 weeks old, 260–300 g body weight) were purchased from Charles River Laboratory Japan (Yokohama, Japan) and were kept in an experimental animal room with an ambient temperature of 22–24°C and a 12-h light–dark cycle for 6 days before use. The cannulated rats were shipped to our lab from Charles River Laboratory Japan 2 days after the surgical procedure and arrived the next day. The *in vivo* and *in situ* studies were conducted on the 9–11th day after the surgery. At 9th day, there observed no significant differences in the physiological condition of cannulated and untreated rats [17].

Surgical Procedure for Portal Vein Cannulation

The surgical procedure for insertion of catheter was used our reported techniques, previously [9,17]. Animals were implanted with catheters in the portal vein as follows. Rats were anaesthetized with ketamine (42.9 mg/kg) and xylazine (8.2 mg/kg) administered intraperitoneally. A mid-line incision 1–2 cm was made in the abdominal cavity and the portal vein was detached near the liver. To prevent bleeding, the portal vein was ligated temporarily as the catheter was inserted. The catheter (3.5Fr polyurethane tube, Access™ technologies Inc.) was inserted immediately and fixed by a purse-string suture on the portal vein. The time to reperfusion was about 1 min after intercepted blood flow. This method for insertion of catheter can avoid the occlusion of the vessel. In addition, a catheter with trumpet-shaped opening was used to prevent the catheter from slipping out of the vessel with minimizing the effect on blood flow. Another end of the catheter was passed subcutaneously to the dorsal base of the neck and the laparotomy was closed in two layers, with a 4/0 silk blade to the muscle, and a surgical clip to close the skin. Surgical procedures were approved by the Institutional Animal Care and Use Committee of Charles River Laboratory Japan. This surgical procedure allows the collection of blood samples without the necessity of restraints and anesthesia.

Blood / Plasma concentration Ratio

The blood / plasma concentration ratio (R_p) was determined *in vitro* after incubation of the compounds with fresh pooled blood from 4 cannulated rats. Blood was preincubated at 37°C in a water bath, and spiked with the test compounds at 100 ng/mL. The blood samples were incubated at 37°C for 15 min. After centrifugation at 14,000g for 10 min, the plasma samples were transferred into 4 volumes of methanol containing ketoconazole (I.S.) and then centrifuged. The concentrations of test compounds in the supernatant were determined

by liquid chromatography / tandem mass spectrometry (LC-MS/MS).

Oral Administration Studies

In order to assess the impact of intestinal metabolism in inhibition method, CYP3A substrates (MDZ, FEL, BUS) and non-metabolizing compound (FEX) were orally administered to the fasted rats (MDZ; 1 mg/kg, FEL; 5 mg/kg, BUS; 3 mg/kg, and FEX; 5 mg/kg) 15 h after oral administration of vehicle or inhibitor (ABT; 100 mg/kg). Dosing regimen of ABT was referred to previous reports [10]. Since ABT is a nonspecific and non-reversible inhibitor of CYP enzymes, inhibitory effect of ABT is sustained and is kept stable for a long time until the enzymes are newly synthesized. In order to assess the impact of intestinal metabolism in distribution method, UGT1a substrate (RLX, 0.98 and 9.8 μ mol/kg) was orally administered to the fasted rats. Each of the model drugs and inhibitors was suspended in aqueous 0.5% methyl cellulose as follows: MDZ, 0.2 mg/mL; FEL, 1 mg/mL; BUS, 0.6 mg/mL; RLX, 0.196 and 1.96 mmol/L; and ABT, 20 mg/mL and the suspension of 5 mL/kg was administered to each rat. Following administration, blood samples were taken from the portal and caudal veins of the unanesthetized rats at 0.083, 0.25, 0.5, 1, 2, 4, 6, and 8 h under unrestricted conditions. In the case of MDZ and BUS, an extra sampling point was added at 0.05 h. The plasma samples were separated by centrifugation at 14,000g for 10 min at 4°C and stored at –30°C until use. The concentrations of unchanged form and metabolites in the plasma were quantified using LC-MS/MS.

Preparation of Perfusate

RLX was dissolved completely in dimethyl sulfoxide (DMSO), then mixed with a solution containing ethanol, cremophor EL, and 0.1 mol/L phosphate buffer adjusted to pH 6.5 (DMSO : ethanol : cremophor : phosphate buffer = 0.5 : 0.25 : 0.25 : 99). Final concentrations of the drug were adjusted to 98 μ mol/L for RLX and 53 μ mol/L for ANT. ANT was added to the perfusate to calculate the portal blood flow for anesthetized individual animals.

In situ Intestinal Single-Pass Perfusion Experiment

The perfusion study was performed according to a previously described method [18,19]. Under anesthesia with 3–4% isoflurane, an incision was made in the abdomens of portal vein-cannulated rats. The length of the perfusion segment was set at approximately 10 cm of upper jejunum, and both ends of the jejunal loop were cannulated with Tygon® flexible plastic tubing (3 mm I.D., and 4 mm O.D.) (Saint-Gobain, Tokyo,

Japan) after flushing out the intestinal contents with warmed physiological saline. The perista pump was connected to the upper tubing and the jejunal loop was perfused with perfusate adjusted to pH 6.5 at a flow rate of about 0.2 mL/min. The flow rate was precisely calculated by measuring weight of collected perfusate from lower tubing. The blood was taken from the peripheral and portal veins at 10 min intervals and the perfusate was collected every 10 min for 1 h.

Dose Number of RLX

The solubility in the intestine may be expressed as Dose Number, which is calculated as the theoretical concentration of RLX in the drug solution (0.1 mg/mL at 0.98 μ mol/kg, 1.0 mg/mL at 9.8 μ mol/kg) divided by solubility. The solubility of RLX was measured as 0.013 mg/mL in the previous report [20].

LC-MS/MS Analysis

The LC-MS/MS system consisted of a HTC PAL autosampler (CTC Analytics, Zwingen, Switzerland), Accela HPLC and TSQ Ultra mass spectrometer (Thermo Fisher Scientific, San Jose, CA). LC conditions were as follows: column, YMC-Triart C18 (2.0 mm I.D. \times 30 mm, 3 μ m; YMC, Kyoto, Japan); column temperature, 40°C; gradient elution at 0.3 mL/min with methanol / aqueous 0.1% formic acid; and injection volume, 15 μ L. The main working parameters for mass spectrometers were as follows: ion mode, electrospray ionization, positive; spray voltage, 4,000 V; sheath gas pressure, 30 arbitrary units (Arb); auxiliary gas pressure, 35 Arb; capillary temperature, 300°C; multireaction monitoring method with transitions of m/z 326.1 \rightarrow 291.1 for MDZ, m/z 342.1 \rightarrow 203.1 for 1-OH-MDZ, m/z 342.1 \rightarrow 234.1 for 4-OH-MDZ, m/z 384.1 \rightarrow 338.0 for FEL, m/z 382.1 \rightarrow 354.1 for D-FEL, m/z 386.3 \rightarrow 122.2 for BUS, m/z 402.3 \rightarrow 139.0 for 6-OH-BUS, m/z 502.3 \rightarrow 466.3 for FEX, m/z 474.2 \rightarrow 112.1 for RLX, m/z 650.2 \rightarrow 474.3 for R6G and R4'G, m/z 189.1 \rightarrow 77.1 for ANT and m/z 531.3 \rightarrow 243.9 for ketoconazole (I.S.). The lower limit of determination was 0.2 or 1 ng/mL and the linear detection range was up to 500 ng/mL. For RLX and ANT, ng/mL converted to nmol/L.

Statistics

The presented values are all mean \pm standard deviation (S.D.). The statistical significance of the difference between mean values was tested using Student's *t* test. Differences with a *p* value of less than 0.05 were considered to be statistically significant.

Data Analysis for Estimation of Intestinal Availability (Fa·Fg)

The mass of drug measured in portal blood (M_{pv}) is taken as the sum of the contribution of intestinal absorption (M_a) and the mass of drug returned to the portal vein from the systemic circulation (M_{sys}).

$$M_{pv} = M_a + M_{sys} \quad (1)$$

M_{pv} and M_{sys} are expressed as

$$M_{pv} = Q_{pv} \times R_b \times AUC_{pv} \quad (2)$$

$$M_{sys} = Q_{pv} \times R_b \times AUC_{sys} \quad (3)$$

where Q_{pv} , R_b , AUC_{pv} and AUC_{sys} are the portal blood flow, the blood / plasma concentration ratio, AUC in the portal vein and in the systemic circulation, respectively. Q_{pv} was calculated as 32.9 mL/min/kg using antipyrine in our previous studies [17]. Then, the total amount of the drug absorbed from GI tract into the portal vein is expressed as

$$M_a = M_{pv} - M_{sys} = Q_{pv} \times R_b \times (AUC_{pv} - AUC_{sys}) \quad (4)$$

Finally, $Fa \cdot Fg$ of drugs were calculated by Eq. (5) which was reported by Hoffman *et al.* [21].

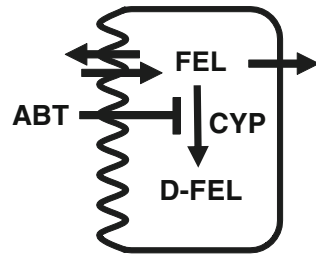
$$Fa \cdot Fg = \frac{M_a}{Dose} = \frac{Q_{pv} \times R_b \times (AUC_{pv} - AUC_{sys})}{Dose} \quad (5)$$

Data analysis for Enzyme-inhibition Method

In this method, as shown in Fig. 1a, intestinal metabolism of CYP3A was inhibited by the pretreatment with ABT. $Fa \cdot Fg$ of drugs in control and ABT-pretreated rats were calculated using Eq. (5). Assuming that ABT completely inhibited the intestinal metabolism by CYP3A (thus $Fg_{ABT} = 1$ in ABT-pretreated rats), Fa can be calculated from Eq. (5). Fg was obtained by dividing $Fa \cdot Fg$ in control rats by $Fa \cdot Fg_{ABT}$ in ABT-treated rats.

$$Fg = \frac{Fa \cdot Fg}{Fa \cdot Fg_{ABT}} \quad (6)$$

a) Enzyme-inhibition method



b) Metabolite-distribution method

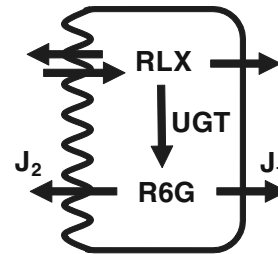


Fig. 1 Schematic diagram of mechanism in enterocytes for Enzyme-inhibition method (a) and Metabolite-distribution method (b). ABT, I-aminobenzotriazole; FEL, felodipine; D-FEL, dehydrofelodipine; RLX, raloxifene; R6G, raloxifene-6-glucuronide; J_1 , absorption rate of R6G; and J_2 , secretion rate of R6G.

Data Analysis for Metabolite-distribution Method

As shown in Fig. 1b, after oral administration of RLX, RLX taken up into enterocyte was mainly metabolized to R6G. Then, the generated R6G in the enterocyte was secreted to the GI tract or absorbed to the portal vein. Amount of absorbed R6G to portal vein was calculated by Eq. (7) in oral administration study of RLX.

$$(\text{Amount of absorbed R6G}) = Q_{pv} \times R_{b, R6G} \times (AUC_{pv, R6G} - AUC_{sys, R6G}) \quad (7)$$

where $R_{b, R6G}$, $AUC_{pv, R6G}$ and $AUC_{sys, R6G}$ are R_b of R6G, AUC of R6G in the portal vein and the systemic circulation, respectively. Amount of secreted R6G was calculated using proportion of secretion rate (J_2) to absorption rate (J_1).

$$(\text{Amount of secreted R6G}) = (\text{Amount of absorbed R6G}) \times J_2/J_1 \quad (8)$$

$$(\text{Total amount of R6G generated in enterocytes}) = (\text{Amount of secreted R6G}) + (\text{Amount of absorbed R6G}) \quad (9)$$

Then, F_g and F_a of RLX was calculated by Eqs. (5), (10) and (11).

$$F_g = 1 - \frac{(\text{Total amount of R6G generated in enterocytes})}{\text{Dose of RLX}} \quad (10)$$

$$F_g = \frac{F_a \cdot F_g}{F_g} \quad (11)$$

J_1 and J_2 of R6G were estimated from *in situ* single-pass perfusion experiments using following Eqs. (12) and (13).

$$J_1 = Q_{pv, ANT} \times R_{b, R6G} \times (C_{pv, R6G} - C_{sys, R6G}) \quad (12)$$

$$J_2 = Q_{lumen} \times C_{out, R6G} \quad (13)$$

where $C_{pv, ANT}$, Q_{lumen} , $C_{pv, R6G}$, $C_{sys, R6G}$, and $C_{out, R6G}$ are the portal blood flow calculated from Eq. (14), the flow rate of perfusion, and concentrations of R6G in the portal and systemic plasma and at exit of jejunal segment, respectively. Both members of following equation represented amount of absorbed ANT from GI tract.

$$Q_{pv, ANT} \times R_{b, ANT} \times (C_{pv, ANT} - C_{sys, ANT}) = Q_{lumen} \times (C_{in, ANT} - C_{out, ANT}) \quad (14)$$

Fig. 2 Systemic (a) and portal (b) plasma concentration-time profiles after oral administration of FEX (5 mg/kg) in control (○) and ABT-pretreated (●) rats. Each value represents the mean + S.D. for 3 to 4 rats.

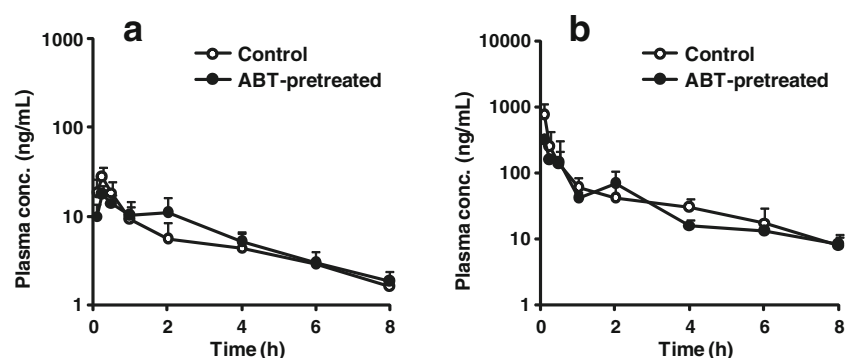


Table 1 The systemic and portal AUCs and $F_a \cdot F_g$ of FEX, MDZ, FEL and BUS after oral administration of FEX (5 mg/kg), MDZ (1 mg/kg), FEL (5 mg/kg), and BUS (3 mg/kg) in control and ABT-Pretreated rats

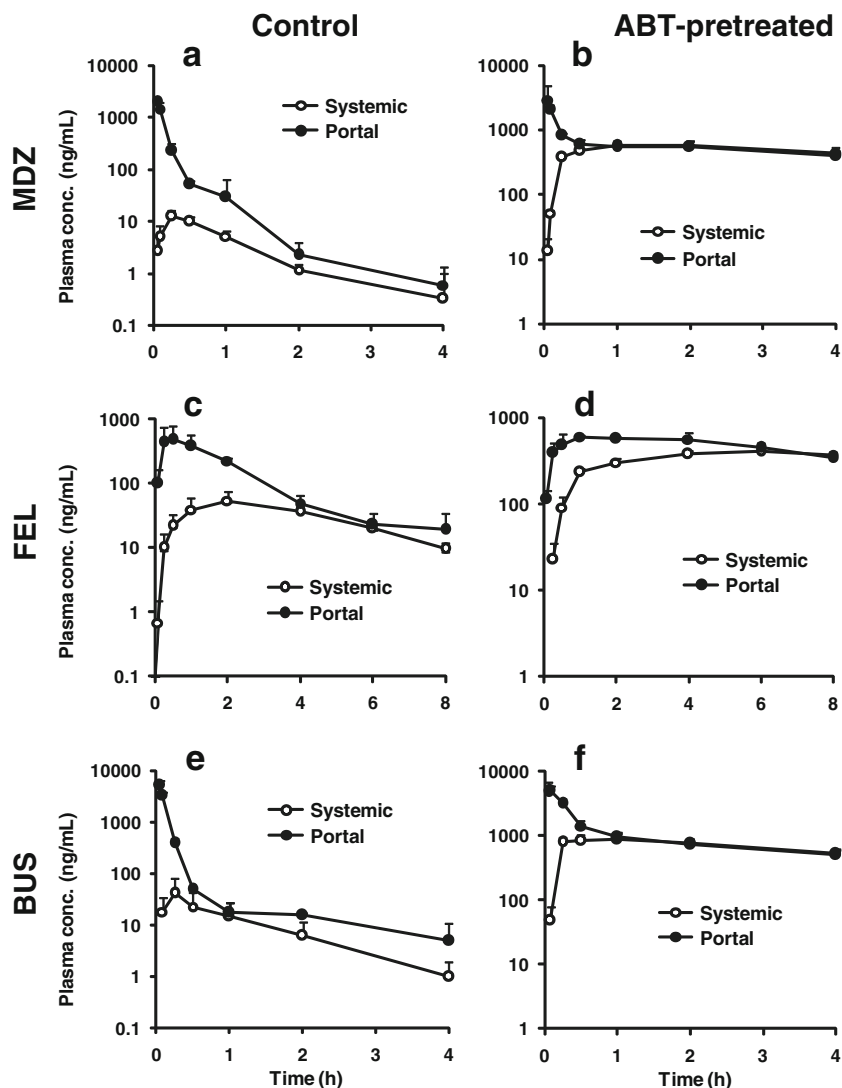
Compound	Dose (mg/kg)	R_b	Control		$F_a \cdot F_g$	ABT-pretreated		$F_a \cdot F_{gABT}$
			AUC_{sys} (ng·h/mL)	AUC_{pv} (ng·h/mL)		AUC_{sys} (ng·h/mL)	AUC_{pv} (ng·h/mL)	
FEX	5	0.99	46.1±8.3	404±23	0.14±0.01	51.7±13.6	324±108	0.11±0.04
MDZ	1	1.22	12.8±2.4	322±84	0.74±0.17	980±109**	1,415±67**	1.05±0.15
FEL	5	0.73	244±63	1,069±316	0.24±0.08	2,613±254**	3,968±239**	0.39±0.03
BUS	3	0.86	41.0±36.7	562±61	0.30±0.05	2,826±580**	4,134±722**	0.74±0.09

Values represent the mean ± S.D. for 3 to 4 rats

** $P < 0.01$, as compared to control rats

R_b , ANT ; C_{pv} , ANT ; C_{sys} , ANT ; C_{in} , ANT ; C_{out} , ANT are R_b of plasma and perfusate at the entrance and exit of jejunal segments, respectively.

Fig. 3 Systemic (○) and portal (●) plasma concentration-time profiles of MDZ, FEL and BUS after oral administration of MDZ (1 mg/kg), FEL (5 mg/kg), and BUS (3 mg/kg) in control and ABT-pretreated rats. The plasma concentration-time profiles of MDZ (a), FEL (c) and BUS (e) in control rats. The plasma concentration-time profiles of MDZ (b), FEL (d) and BUS (f) in ABT-pretreated rats. Each value represents the mean ± S.D. for 3 to 4 rats.



RESULTS

Assessment of CYP3A-mediated Intestinal Metabolism with the Enzyme-Inhibition Method

Effect of ABT Pretreatment on the Pharmacokinetics of FEX

In order to evaluate the effects of ABT pretreatment on transporter activity, FEX was orally administered to PV rats after oral pretreatment with 100 mg/kg ABT. FEX is not appreciably metabolized and has low passive permeability, but its absorption and disposition are regulated by P-gp and OATPs [22]. As shown in Fig. 2, the portal and systemic plasma concentration-time profiles of FEX in ABT-pretreated rats were almost the same as those of control rats. As Table I shows, no significant differences were detected in the portal and systemic AUCs of FEX between ABT-pretreated and control rats. As a result, $F_a \cdot F_g$ of FEX was calculated to be the same between both rats (0.14 ± 0.01 in control rats, 0.11 ± 0.04 in ABT-pretreated rats), suggesting that ABT has no effects on transporters that mediate the absorption and disposition of FEX.

Intestinal Metabolism of CYP3A Substrate Drugs

As shown in Table I and Fig. 3, the portal and systemic AUCs of the unchanged form after oral administration of model drugs (MDZ, FEL and BUS) in ABT-pretreated rats were significantly higher than those of control rats, indicating that intestinal and hepatic CYP3A-mediated metabolism were inhibited by ABT pretreatment. Thus, $F_a \cdot F_{gABT}$ of CYP3A substrates in ABT pretreated-rats became higher than those of controls.

Table II and Fig. 4 show that the portal plasma concentration and the portal AUC of the main metabolites of model drugs (1-OH-MDZ, 4-OH-MDZ, D-FEL, and 6-OH-BUS) in control rats were higher than those in systemic plasma after oral administration of their parent drugs. In the case of 4-OH-MDZ and 6-OH-BUS, the difference between portal and systemic AUC was not significant. ($p=0.053$ for 4-OH-MDZ, $p=0.050$ for 6-OH-BUS). As a reason of no significant differences, existence of multiple pathways of metabolism for these drugs might make it difficult to detect the difference statistically [23].

In contrast, in ABT-pretreated rats, the portal and systemic plasma concentration-time profiles of each metabolite were essentially superimposable and AUCs of both plasma concentrations were consistent. Because the difference between the portal and systemic plasma concentration represents the plasma concentration of metabolites generated by first-pass metabolism in the intestine, this result clearly suggests that

Table II The systemic and portal AUCs of 1-OH-MDZ, 4-OH-MDZ, D-FEL and 6-OH-BUS after oral administration of MDZ (1 mg/kg), FEL (5 mg/kg), and BUS (3 mg/kg) in control and ABT-pretreated rats

Metabolite Parameter	Interval (h)	Control	ABT-pretreated
1-OH-MDZ			
AUC _{sys} (ng·h/mL)	0–4	6.34±1.56	184±33
AUC _{pv} (ng·h/mL)		21.3±3.0**	172±16
4-OH-MDZ			
AUC _{sys} (ng·h/mL)	0–0.5	1.39±0.34	1.16±0.60
AUC _{pv} (ng·h/mL)		3.57±1.18	1.60±0.93
D-FEL			
AUC _{sys} (ng·h/mL)	0–8	26.1±13.8	251±118
AUC _{pv} (ng·h/mL)		245±60**	289±106
6-OH-BUS			
AUC _{sys} (ng·h/mL)	0–0.5	46.9±10.9	8.48±1.67
AUC _{pv} (ng·h/mL)		103±33	12.1±2.8

Values represent the mean ± S.D. for 3 to 4 rats

** $P < 0.01$, as compared to AUC_{sys}

CYP3A-mediated metabolism in enterocytes was inhibited almost completely by ABT pretreatment. When intestinal CYP3A-mediated metabolism was completely inhibited by ABT pretreatment, F_a was calculated from Eq. (5) by assuming $F_{gABT} = 1$ in ABT-pretreated rats, and F_g was obtained by dividing $F_a \cdot F_g$ in control rats by $F_a \cdot F_{gABT}$ in ABT-pretreated rats.

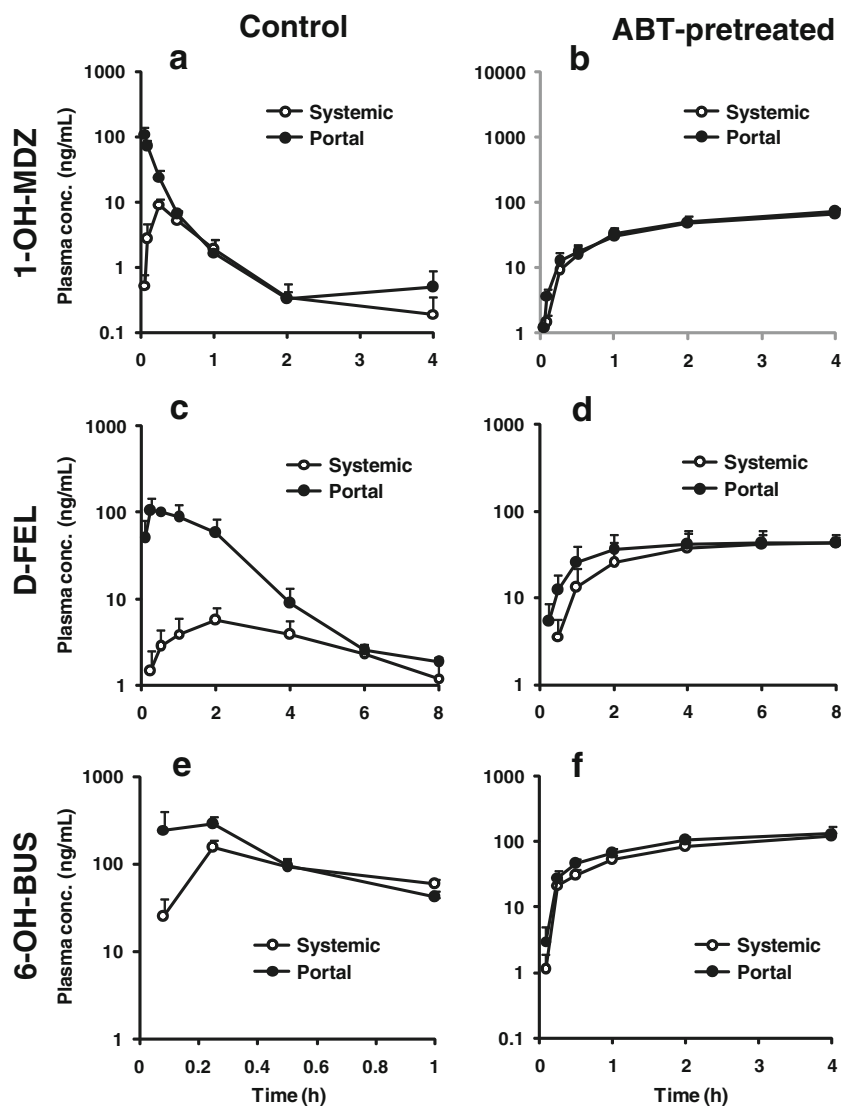
Estimated values of F_a for FEX, MDZ, FEL, and BUS using this Enzyme-inhibition method were 0.11 ± 0.04 , 1.05 ± 0.15 , 0.39 ± 0.03 , and 0.74 ± 0.09 , respectively and were well correlated with those of previous reports that employed Caco-2 cell lines (Table III). The F_g of FEX was calculated as 1 since $F_a \cdot F_{gABT}$ of FEX was the same as $F_a \cdot F_g$ in control rats. The calculated values of F_g for MDZ, FEL, and BUS were 0.71, 0.61, and 0.40, respectively.

Assessment of UGT-mediated Intestinal Metabolism with the Metabolite-Distribution Method

Pharmacokinetics of RLX and its Glucuronide

In order to assess F_a , F_g and $F_a \cdot F_g$ of RLX, which is metabolized by UGT but not CYP in rat intestinal microsomes [24], RLX, R4'G, and R6G concentrations in portal and systemic plasma were determined using synthetic standards after oral administration of RLX (9.8 μmol/kg) to PV rats. As shown in Fig. 5a, the systemic plasma concentration of R6G was approximately 2 to 14 times higher than that of unchanged RLX

Fig. 4 Systemic (○) and portal (●) plasma concentration-time profiles of 1-OH-MDZ, D-FEL and 6-OH-BUS after oral administration of MDZ (1 mg/kg), FEL (5 mg/kg), and BUS (3 mg/kg) in control and ABT-pretreated rats. The plasma concentration-time profiles of 1-OH-MDZ (a), D-FEL (c) and 6-OH-BUS (e) in control rats. The plasma concentration-time profile of 1-OH-MDZ (b), D-FEL (d) and 6-OH-BUS (f) in ABT-pretreated rats. Each value represents the mean + S.D. for 3 to 4 rats.



at each sampling point. R6G is reported to be a major metabolite in rat intestinal and liver microsomes [14]. Since

Table III Fa·Fg, Fa and Fg of FEX, MDZ, FEL and BUS after oral administration of FEX (5 mg/kg), MDZ (1 mg/kg), FEL (5 mg/kg), and BUS (3 mg/kg) in the PV rats

Compound	Dose (mg/kg)	Fa·Fg	Fa	Fg	$P_{app, \text{caco-2}}$ (10^{-6} cm/s)
FEX	5	0.14 ± 0.01	0.11 ± 0.04	1.00	0.17^a
MDZ	1	0.74 ± 0.17	1.05 ± 0.15	0.71	32.4^b
FEL	5	0.24 ± 0.08	0.39 ± 0.03	0.61	4.2^b
BUS	3	0.30 ± 0.05	0.74 ± 0.09	0.40	25.4^b

Fg of FEX was assumed to be 1

Values represent the mean \pm S.D. for 3 to 4 rats

^a The data was obtained from a report by Petri N *et al.* [32]

^b The data was obtained from a report by Gertz M *et al.* [33]

the amount of absorbed R6G calculated by Eq. (7) was 13 times higher than that of R4'G (Table IV, 1.43 ± 0.26 $\mu\text{mol/kg}$ for R6G, 0.11 ± 0.01 $\mu\text{mol/kg}$ for R4'G), the contribution of metabolism to R4'G in overall intestinal metabolism was considered to be negligible. Fa·Fg of RLX was 0.15 ± 0.12 , and 0.18 ± 0.03 at doses of 0.98, and 9.8 $\mu\text{mol/kg}$, respectively. As shown in Fig. 5c, the differences between portal and systemic plasma concentrations of R6G became nearly constant at 30 min after administration of RLX, suggesting that RLX was metabolized to R6G at a constant rate in enterocytes.

Estimation of Portal Blood Flow during In Situ Rat Single-Pass Perfusion of ANT

ANT was perfused into rat jejunum with RLX to estimate individual portal blood flow using eq. (14) since ANT is highly and rapidly absorbed by passive diffusion, and Fg and Fh of

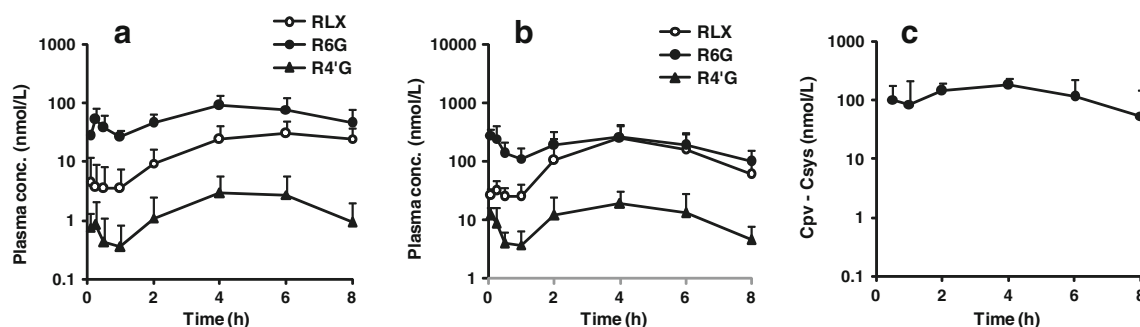


Fig. 5 Systemic (a) and portal (b) plasma concentration-time profile of RLX (○), R6G (●), and R4'G (▲) and difference between systemic and portal plasma concentration of R6G (c) after oral administration of RLX (9.8 $\mu\text{mol/kg}$) in the PV rats. Each value represents the mean + S.D. for 5 rats.

ANT can be assumed to be almost 1 [25]. As shown in Fig. 6, the portal concentration of ANT was higher than the systemic concentration, and both portal and systemic plasma concentration gradually increased during the experiment. However the difference in concentration between the two was nearly constant, suggesting that the ANT absorption process rapidly reached a steady state within 10 min following perfusion. Moreover, Table V shows that the difference in perfusate concentration between the entrance and exit of jejunal segments was also nearly constant and that a calculated portal blood flow from 10 to 60 min after starting perfusion was 17.1 to 22.4 mL/min/kg.

Distribution of R6G following In Situ Rat Single-Pass Perfusion of RLX

After perfusion of RLX, the portal concentration of R6G was higher than the systemic concentration, with the difference between them nearly constant (Fig. 7), indicating that the perfused RLX was metabolized to R6G at a constant rate in enterocytes. As shown in Fig. 1b, RLX taken up into the intestinal mucosa was metabolized mainly to R6G in the cells, and R6G was then transported into both the intestinal lumen

and the mesenteric vein. The proportion of the secretion rate (J_2) to absorption rate (J_1) of R6G from enterocytes was evaluated by an *in situ* single-pass perfusion experiment. J_1 and J_2 were estimated by Eqs. (12) and (13), respectively. As shown in Fig. 8, the J_2 / J_1 ratio was nearly constant during the experiment. The rate of transport of R6G into the intestinal lumen (J_2) was 2.33-fold faster than into the blood (J_1).

Intestinal Metabolism of UGT Substrate drug

The Fg of RLX was calculated from both an oral administration study and an *in situ* single-perfusion experiment. It was assumed that the J_2 / J_1 ratio of R6G in the *in situ* single-perfusion experiment was the same as that in the oral administration study since the surface area of the brush border membrane and the expression of efflux transporters that influence the distribution of R6G in enterocytes were the same in both studies. As shown in Table VI, Fa and Fg of RLX were 0.74 and 0.21 at 0.98 $\mu\text{mol/kg}$, and 0.35 and 0.51 at 9.8 $\mu\text{mol/kg}$, respectively. The Dose Number of RLX in humans was reported as 18 by Benet *et al.* [20]. In this study, the Dose Number of RLX was 8 at 0.98 $\mu\text{mol/kg}$, and 80 at 9.8 $\mu\text{mol/kg}$.

Table IV The systemic and portal AUCs and Fa·Fg of RLX after oral administration of RLX (0.98 and 9.8 $\mu\text{mol/kg}$) in the PV rats

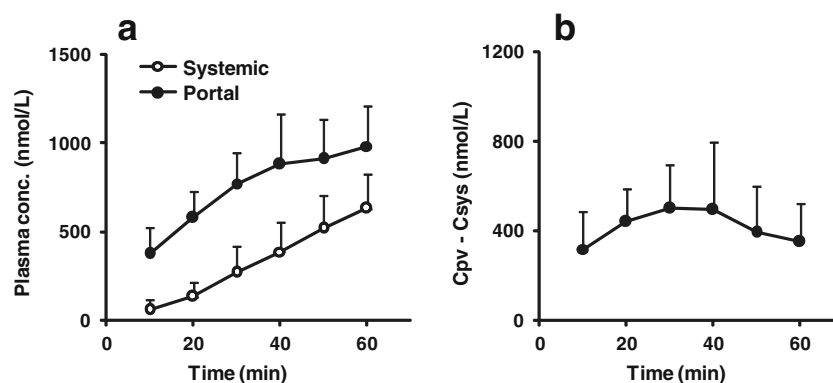
Species	Compound Metabolite	Dose ($\mu\text{mol/kg}$)	Dose Number	R_b	AUC _{sys} (nmol·h/L)	AUC _{pv} (nmol·h/L)	Absorbed metabolite ($\mu\text{mol/kg}$)	Fa·Fg
Rat	RLX	0.98	8	0.96	8.27±2.99	87.8±63.3	-	0.15±0.12
	R6G			0.70	47.6±8.7	216±80	0.23±0.10	-
	RLX	9.8	80	0.96	153±72	1,089±220	-	0.18±0.03
	R6G			0.70	496±137	1,532±193	1.43±0.26	-
	R4'G			0.70	14.6±6.8	95.9±13.7	0.11±0.01	-
Human	RLX	1.96	18 ^a	-	-	-	-	0.034 ^b

Values represent the mean ± S.D. for 5 rats

^a The data was obtained from a report by Benet LZ *et al.* [20]

^b The data was obtained from a report by Mizuma *et al.* [6]

Fig. 6 Systemic (○) and portal (●) plasma concentration-time profiles of ANT (**a**), and difference between systemic and portal plasma concentration of ANT (**b**) in a rat jejunal single-pass perfusion experiment. Each value represents the mean + S.D. for 7 rats.



DISCUSSION

Although the total amount of CYP3A expressed in human small intestine represents approximately 1% of the hepatic estimate [26], considerable drug extraction occurs during absorption of orally administered drugs [27,28]. Likewise, intestinal metabolism by UGT has been reported to significantly contribute to first-pass effects [6,16]. In the process of drug development, it is important to determine the contribution of these metabolic enzymes in overall absorption because this quantitative information helps in the further understanding of pharmacokinetics in laboratory animals and in humans.

Because the impact of intestinal metabolism is influenced not only by intrinsic metabolic activity but also by physiological complexities such as luminal pH, luminal volume, surface area, and localization of metabolic enzymes, the prediction of Fg from *in vitro* data alone has not been fully validated. Yang *et al.* [29] established the Q_{gut} model for intestinal metabolism of CYP3A substrates, which takes into account the interplay between permeability and metabolism; and additionally, several improved methods based on the Q_{gut} model have been reported [4,30]. The simplified intestinal availability (SIA) model reported by Kadono *et al.* [30], which utilizes only intrinsic metabolic activity, enabled the prediction of Fg of not only CYP3A substrates but also UGT substrates with high permeability, which are assumed to undergo complete

absorption (Fa = 1) [24]. For compounds with low permeability or low solubility, however, the SIA model overestimates the impact of intestinal metabolism. On the other hand, in order to estimate Fg *in vivo*, co-administration studies with metabolic inhibitors such as grapefruit juice and ketoconazole are often carried out using experimental animals. In this approach, if systemic clearance of the test compound is altered by the metabolic inhibitors, an intravenous study is required for each inhibitor dose. We previously reported that PV rats enabled estimation of the effects of selective inhibitors only through an oral administration study, independently of variable systemic clearance [9]. In this study, using the Enzyme-inhibition method with ABT enabled assessment of the quantitative contribution of intestinal CYP3A-mediated metabolism and allowed separate assessments of Fa and Fg.

In this method, the effect of inhibitor should be selective for CYP-mediated metabolism because many compounds are dual substrates for P-gp and CYP3A. The portal and systemic plasma concentration-time profiles of FEX were almost the same between control and ABT-pretreated rats. Since we have already shown that 71% of FEX taken up into enterocytes is effluxed to the apical surface by P-gp [9], it was concluded that ABT has no effects on the activity of P-gp and OATP which mediate the absorption and disposition of FEX. Strelevitz *et al.* [10] also reported that the systemic plasma concentration of FEX was not affected by ABT pretreatment.

When CYP3A substrate drugs (MDZ, FEL and BUS) were orally administered, the portal AUC of their metabolites was significantly higher than the systemic AUC in control rats, whereas the portal and systemic plasma concentration-time profiles of the metabolites were almost the same in ABT-pretreated rats. These data suggest that intestinal CYP3A-mediated metabolism is inhibited almost completely by ABT pretreatment. Hepatic metabolism might not be inhibited completely since metabolites were detected in the plasma of ABT-pretreated rats.

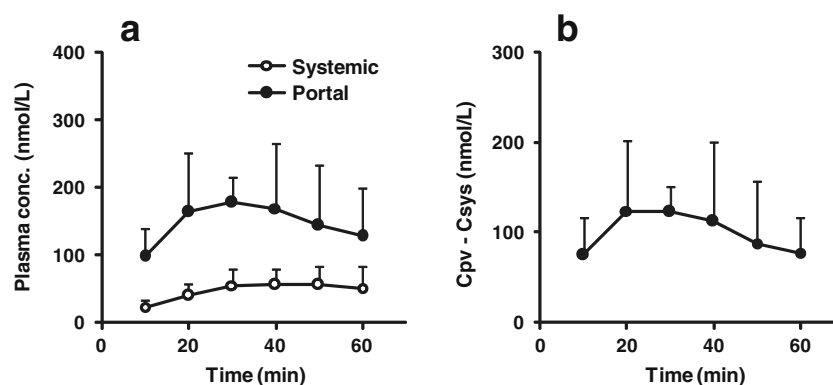
The Fg of MDZ in rats was reported to be 0.75 using *in situ* mesenteric blood-collecting method [31] and 0.57 in a perfused everted intestinal segment study [32]. Our result (Fg =

Table V The calculated portal blood flow from perfusate and plasma concentrations of ANT in a rat jejunal single-pass perfusion experiment

Time (min)	C _{in, ANT} - C _{out, ANT} (μmol/L)	C _{pv, ANT} - C _{sys, ANT} (nmol/L)	Q _{pv, ANT} (mL/min/kg)
10	9.79 ± 4.11	367 ± 118	22.1 ± 14.6
20	14.4 ± 6.1	501 ± 211	22.4 ± 13.4
30	12.0 ± 5.3	453 ± 126	18.5 ± 8.6
40	11.4 ± 4.3	520 ± 266	19.6 ± 12.1
50	10.1 ± 3.5	390 ± 153	20.3 ± 9.5
60	8.04 ± 3.55	398 ± 203	17.1 ± 12.7

Values represent the mean ± S.D. for 7 rats

Fig. 7 Systemic (○) and portal (●) plasma concentration-time profiles of R6G (**a**), and difference between systemic and portal plasma concentration of R6G (**b**) in a rat jejunal single-pass perfusion experiment. Each value represents the mean + S.D. for 7 rats.



0.71) agrees with these reports. The reported permeability of FEX, MDZ, FEL, and BUS in the Caco-2 cell line was 0.17, 32.4, 4.2, and 25.4×10^{-6} cm/s, respectively [33,34]. The absorbed fraction following oral drug administration correlates well in a sigmoidal manner with Caco-2 cell permeability [35], suggesting support for our results as well.

In the *in situ* intestinal perfusion study, the J_2/J_1 of R6G was calculated as 2.33, indicating that this metabolite is transported preferentially to the intestinal lumen rather than the mesenteric vein. Temocapril, an angiotensin-converting enzyme inhibitor, is hydrolyzed to temocaprilat in the intestine and liver. Nozawa and Imai [19] reported that in an *in situ* rat jejunal perfusion model, temocaprilat formed from enterocytes was transported approximately 2-fold faster into the lumen than into the mesenteric vein when the luminal and venous fluid were at pH 6.4 and 7.4, respectively. The reason for this phenomenon was speculated to be the larger surface area of the brush border membrane due to the presence of microvilli compared to the basolateral membrane. Likewise, in the perfusion experiment with ethyl-FEX, the ester prodrug

of FEX, the rate of transport of FEX into the lumen was 4.6-fold faster than that into the blood [36]. With regard to FEX, the efflux of FEX *via* P-gp in addition to passive diffusion appears to be responsible for the more rapid transport of FEX. Therefore, it is reasonable that efflux of R6G into the lumen may be mediated by passive as well as active transport, since excretion of R6G was influenced by MRP2 [15,16].

In this study, the rate of transport of R6G (J_1) into the mesenteric vein was corrected by individual portal blood flow estimated by single-perfusion of ANT. As shown in Table V, due to the effects of laparotomy and anesthesia, the calculated portal blood flow was lower than that stated in our previous report (32.9 mL/min/kg) under free-moving conditions.

Using the Metabolite-distribution method, the Fa of RLX after oral administration at 0.98 and 9.8 $\mu\text{mol/kg}$ was determined as 0.74 and 0.35, respectively. Fa of RLX in humans is reported to be 0.63 [6], which is similar to that of rat at 0.98 $\mu\text{mol/kg}$. As shown in Table IV, Dose Number of RLX in humans was similar compared to low dose in rats (0.98 $\mu\text{mol/kg}$). On the other hand, Dose Number at 9.8 $\mu\text{mol/kg}$ was extensively high, suggesting that the orally administered RLX did not completely dissolve in the GI tract. In addition, Fg of RLX at 0.98 $\mu\text{mol/kg}$ was lower than that at 9.8 $\mu\text{mol/kg}$, and the ratio of R6G absorbed from enterocytes to RLX administered was higher at 0.98 $\mu\text{mol/kg}$, indicating that intestinal UGT involved in the metabolism of RLX might be saturated at 9.8 $\mu\text{mol/kg}$.

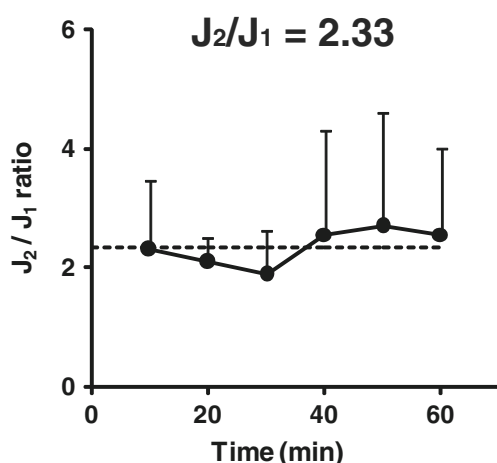


Fig. 8 The proportion of secretion rate (J_2) to absorption rate (J_1) of R6G from enterocytes in a rat jejunal single-pass perfusion experiment. The dotted line represented the average value of J_2/J_1 . The average J_2/J_1 from 10 to 60 min was 2.33. Each value represents the mean + S.D. for 7 rats.

Table VI The Fa·Fg, Fa, and Fg of RLX after oral administration of RLX in the PV rats and human

Species	Dose ($\mu\text{mol/kg}$)	Fa·Fg	Fa	Fg
Rat	0.98	0.15 ± 0.12	0.74	0.21
	9.8	0.18 ± 0.03	0.35	0.51
Human	1.96	0.034^a	0.63^a	0.054^a

Values represent the mean \pm S.D. for 5 rats

^a The data was obtained from a report by Mizuma et al. [6]

CONCLUSIONS

The PV rats used in this study enabled quantitative assessment of the contribution of intestinal CYP3A-mediated metabolism to the oral bioavailability of model drugs using the Enzyme-inhibition method with ABT. Furthermore, if a selective inhibitor for an intestinal metabolizing enzyme has not been identified, it is possible to apply the Metabolite-distribution method to evaluate the impact of intestinal first-pass metabolism. These experimental methods are useful for clarifying the cause of low bioavailability of new drug candidates during the drug discovery stage.

ACKNOWLEDGMENTS & DISCLOSURES

We thank Kunihiko Morisaki (Charles River Laboratories Japan), Dr. Jiro Kuze (Taiho Pharmaceutical Co. Ltd.), and Dr. Toshiyuki Kume (Mitsubishi Tanabe Pharma Corporation) for useful discussions.

REFERENCES

- Wilkinson GR. Drug metabolism and variability among patients in drug response. *N Engl J Med*. 2005;352:2211–21.
- Watkins PB, Wrighton SA, Schuetz EG, Molowa DT, Guzelian PS. Identification of glucocorticoid-inducible cytochromes P-450 in the intestinal mucosa of rats and man. *J Clin Invest*. 1987;80:1029–36.
- Paine MF, Hart HL, Ludington SS, Haining RL, Rettie AE, Zeldin DC. The human intestinal cytochrome P450 “pie”. *Drug Metab Dispos*. 2006;34:880–6.
- Nishimuta H, Sato K, Yabuki M, Komuro S. Prediction of the intestinal first-pass metabolism of CYP3A and UGT substrates in humans from *in vitro* data. *Drug Metab Pharmacokinet*. 2011;26:592–601.
- Williams JA, Hyland R, Jones BC, Smith DA, Hurst S, Goosen TC, *et al*. Drug-drug interactions for UDP-glucuronosyltransferase substrates: a pharmacokinetic explanation for typically observed low exposure (AUCi/AUC) ratios. *Drug Metab Dispos*. 2004;32:1201–8.
- Mizuma T. Intestinal glucuronidation metabolism may have a greater impact on oral bioavailability than hepatic glucuronidation metabolism in humans: a study with raloxifene, substrate for UGT1A1, 1A8, 1A9, and 1A10. *Int J Pharm*. 2009;378:140–1.
- Ogasawara A, Kume T, Kazama E. Effect of oral ketoconazole on intestinal first-pass effect of midazolam and fexofenadine in cynomolgus monkeys. *Drug Metab Dispos*. 2007;35:410–8.
- Nishimuta H, Sato K, Mizuki Y, Yabuki M, Komuro S. Prediction of the intestinal first-pass metabolism of CYP3A substrates in humans using cynomolgus monkeys. *Drug Metab Dispos*. 2010;38:1967–75.
- Matsuda Y, Konno Y, Hashimoto T, Nagai M, Taguchi T, Satsukawa M, *et al*. *In vivo* assessment of the impact of efflux transporter on oral drug absorption using portal vein-cannulated rats. *Drug Metab Dispos*. 2013;41:1514–21.
- Strelevitz TJ, Foti RS, Fisher MB. *In vivo* use of the P450 inactivator 1-aminobenzotriazole in the rat: varied dosing route to elucidate gut and liver contributions to first-pass and systemic clearance. *J Pharm Sci*. 2006;95:1334–41.
- Sun Q, Harper TW, Dierks EA, Zhang L, Chang S, Rodrigues AD, *et al*. 1-Aminobenzotriazole, a known cytochrome P450 inhibitor, is a substrate and inhibitor of N-acetyltransferase. *Drug Metab Dispos*. 2011;39:1674–9.
- Mico BA, Federowicz DA, Ripple MG, Kerns W. *In vivo* inhibition of oxidative drug metabolism by, and acute toxicity of, 1-aminobenzotriazole (ABT). a tool for biochemical toxicology. *Biochem Pharmacol*. 1988;37:2515–9.
- Meschter CL, Mico BA, Mortillo M, Feldman D, Garland WA, Riley JA, *et al*. A 13-week toxicologic and pathologic evaluation of prolonged cytochromes P450 inhibition by 1-aminobenzotriazole in male rats. *Fundam Appl Toxicol*. 1994;22:369–81.
- Jeong EJ, Liu Y, Lin H, Hu M. Species and disposition model-dependent metabolism of raloxifene in gut and liver: role of UGT1A10. *Drug Metab Dispos*. 2005;33:785–94.
- Jeong EJ, Lin H, Hu M. Disposition mechanisms of raloxifene in the human intestinal Caco-2 model. *J Pharmacol Exp Ther*. 2004;310:376–85.
- Kosaka K, Sakai N, Endo Y, Fukuhara Y, Tsuda-Tsukimoto M, Ohtsuka T, *et al*. Impact of intestinal glucuronidation on the pharmacokinetics of raloxifene. *Drug Metab Dispos*. 2011;39:1495–502.
- Matsuda Y, Konno Y, Satsukawa M, Kobayashi T, Takimoto Y, Morisaki K, *et al*. Assessment of intestinal availability of various drugs in the oral absorption process using portal vein-cannulated rats. *Drug Metab Dispos*. 2012;40:2231–8.
- Takahashi M, Washio T, Suzuki N, Igeta K, Yamashita S. Investigation of the intestinal permeability and first-pass metabolism of drugs in cynomolgus monkeys using single-pass intestinal perfusion. *Biol Pharm Bull*. 2010;33:111–6.
- Nozawa T, Imai T. Prediction of human intestinal absorption of the prodrug temocapril by *in situ* single-pass perfusion using rat intestine with modified hydrolase activity. *Drug Metab Dispos*. 2011;39:1263–9.
- Benet LZ, Broccatelli F, Oprea TI. BDDCS applied to over 900 drugs. *AAPS J*. 2011;13:519–47.
- Hoffman DJ, Seifert T, Borre A, Nellans HN. Method to estimate the rate and extent of intestinal absorption in conscious rats using an absorption probe and portal blood sampling. *Pharm Res*. 1995;12:889–94.
- Cvetkovic M, Leake B, Fromm MF, Wilkinson GR, Kim RB. OATP and P-glycoprotein transporters mediate the cellular uptake and excretion of fexofenadine. *Drug Metab Dispos*. 1999;27:866–71.
- Zhu M, Zhao W, Jimenez H, Zhang D, Yeola S, Dai R, *et al*. Cytochrome P450 3A-mediated metabolism of buspirone in human liver microsomes. *Drug Metab Dispos*. 2005;33:500–7.
- Furukawa T, Nakamori F, Tetsuka K, Naritomi Y, Moriguchi H, Yamano K, *et al*. Quantitative prediction of intestinal glucuronidation of drugs in rats using *in vitro* metabolic clearance data. *Drug Metab Pharmacokinet*. 2012;27:171–80.
- Yamashita S, Yoshida M, Taki Y, Sakane T, Nadai T. Kinetic analysis of the drug permeation process across the intestinal epithelium. *Pharm Res*. 1994;11:1646–51.
- Paine MF, Khalighi M, Fisher JM, Shen DD, Kunze KL, Marsh CL, *et al*. Characterization of interintestinal and intrainestinal variations in human CYP3A-dependent metabolism. *J Pharmacol Exp Ther*. 1997;283:1552–62.
- Paine MF, Shen DD, Kunze KL, Perkins JD, Marsh CL, McVicar JP, *et al*. First-pass metabolism of midazolam by the human intestine. *Clin Pharmacol Ther*. 1996;60:14–24.
- Gertz M, Davis JD, Harrison A, Houston JB, Galetin A. Grapefruit juice-drug interaction studies as a method to assess the extent of intestinal availability: utility and limitations. *Curr Drug Metab*. 2008;9:785–95.
- Yang J, Jamei M, Yeo KR, Tucker GT, Rostami-Hodjegan A. Prediction of intestinal first-pass drug metabolism. *Curr Drug Metab*. 2007;8:676–84.
- Kadono K, Akabane T, Tabata K, Gato K, Terashita S, Teramura T. Quantitative prediction of intestinal metabolism in humans from a

- simplified intestinal availability model and empirical scaling factor. *Drug Metab Dispos.* 2010;38:1230–7.
31. Higashikawa F, Murakami T, Kaneda T, Kato A, Takano M. Dose-dependent intestinal and hepatic first-pass metabolism of midazolam, a cytochrome P450 3A substrate with differently modulated enzyme activity in rats. *J Pharm Pharmacol.* 1999;51:67–72.
 32. Hirunpanich V, Murakoso K, Sato H. Inhibitory effect of docosahexaenoic acid (DHA) on the intestinal metabolism of midazolam: *in vitro* and *in vivo* studies in rats. *Int J Pharm.* 2008;351:133–43.
 33. Petri N, Tannergren C, Rungstad D, Lennernäs H. Transport characteristics of fexofenadine in the Caco-2 cell model. *Pharm Res.* 2004;21:1398–404.
 34. Gertz M, Harrison A, Houston JB, Galetin A. Prediction of human intestinal first-pass metabolism of 25 CYP3A substrates from *in vitro* clearance and permeability data. *Drug Metab Dispos.* 2010;38:1147–58.
 35. Artursson P, Karlsson J. Correlation between oral drug absorption in humans and apparent drug permeability coefficients in human intestinal epithelial (Caco-2) cells. *Biochem Biophys Res Commun.* 1991;175:880–5.
 36. Ohura K, Soejima T, Nogata R, Adachi Y, Ninomiya S, Imai T. Effect of intestinal first-pass hydrolysis on the oral bioavailability of an ester prodrug of fexofenadine. *J Pharm Sci.* 2012;101:3264–74.